FEBS 18362 FEBS Letters 405 (1997) 373–377

Engineering of diffraction-quality crystals of the NF-κB P52 homodimer:DNA complex

Patrick Cramer, Christoph W. Müller*

European Molecular Biology Laboratory (EMBL), Grenoble Outstation, c/o ILL, B.P. 156, 38042 Grenoble Cedex 9, France

Received 23 January 1997

Abstract The eukaryotic transcription factors NF-κB P50 and NF-κB P52 are closely related members of the Rel family. Growth of diffraction-quality NF-κB P52:DNA co-crystals crucially depended on (a) extensive screens for the DNA fragment of optimal length and (b) engineering of the protein based on the two known NF-κB P50:DNA co-crystal structures [Müller et al. (1995) Nature 373, 311–317; Ghosh et al. (1995) Nature 373, 303–310]; namely, deletion of 12 C-terminal amino acid residues. These residues are part of the Rel homology region and comprise the nuclear localization signal. The approach might be of general use for the crystallization of other Rel protein: DNA complexes and in our case yielded co-crystals which diffract beyond 2.0 Å resolution.

Key words: Rel protein; NF-κB P52; Protein:DNA interaction; Co-crystallization; Transcription; Protein engineering

1. Introduction

Proteins of the NF-κB/Rel family of eukaryotic transcription factors control many genes that mediate the immune response in mammals and play a major role in gene expression of viruses such as HIV or Herpes [3]. The mammalian NF-κB/Rel family members include P50, P52, P65, RelB and c-Rel [3]. Other family members are the *Drosophila* proteins Dorsal, Dif and Relish [4] as well as the recently discovered protein Gambif1 from *Anopheles gambiae* [5]. The insect proteins are involved in morphogenesis (Dorsal) and primitive immune defense (Dif, Relish and Gambif1). Activity and cellular localization of NF-κB/Rel proteins are regulated through interactions with proteins of the I-κB family [6]. The two independently solved crystal structures of the NF-κB P50 homodimer complexed with DNA at 2.3 and 2.6 Å resolution [1,2] are the first steps in a detailed structure-function analysis of the NF-κB/Rel family [7]. The structures reveal a new mode of DNA binding with the transcription factor dimer wrapped around the DNA.

NF-κB P52 is a close homologue to NF-κB P50. Both proteins are synthesized as precursor molecules P100 and P105, respectively ([3], Fig. 1a). The C-terminal regions of P100 and P105 show I-κB like activity and they are removed proteolytically in vivo to yield NF-κB P52 or P50, respectively [6]. NF-κB P50 and NF-κB P52 contain additional amino acid residues ('insert', Fig. 1) which are not part of the Rel homology region (RHR). They are located within an extension between β-strands G′ and H of the N-terminal domain, which is known as 'insert region'. In NF-κB P50, the insert region comprises 66 residues (Val-145 to Leu-210) and has a compact, mostly α-helical structure. The insert region of NF-κB P52 is 19 amino acid residues shorter (Val-141 to Leu-187). Within the RHR and the insert, NF-κB P50 and NF-κB P52 show 63% sequence identity. Despite the high sequence similarity, NF-κB P50 and NF-κB P52 show differences in DNA-binding specificity [8] and in the specificity of interactions with proteins of the I-κB family [6,9]. To study further the structure and DNA binding of Rel proteins, the determination of the crystal structure of NF-κB P52 in complex with DNA seemed an obvious goal.

To obtain detailed structural information about protein:DNA interactions by X-ray crystallography, the growth of highly ordered three-dimensional co-crystals is a prerequisite. In the search for high-quality co-crystals, badly ordered, weakly diffracting crystals are frequently encountered. In this paper we describe how rational engineering of the protein and variation of the length of the DNA duplexes yielded diffraction-quality co-crystals of the NF-κB P52 homodimer with a 13-mer DNA fragment. Further, we show that these crystals could be transformed to a high-resolution form using a special soaking protocol prior to crystal freezing.

2. Materials and methods

2.1. Protein expression and purification

The protein was isolated from an overproducing strain of *Escherichia coli* (BL21 DE3) harboring the plasmid pLM1 which contains the gene encoding for human NF-κB P52 (construct A, Fig. 1). This plasmid was kindly provided by C.L. Larson and G. Verdine (Harvard University). The expression vector pLM1 uses the bacteriophage T7 promoter and carries ampicillin resistance [10]. Cells were grown at 25°C in 2-l flasks in 0.5 l of LB medium containing 100 μg/ml ampicillin. Expression was induced by addition of IPTG to a concentration of 0.1 mM when $A_{600} = 0.6$ was reached. After induction, cells were grown for another 5 h. All further manipulations were carried out at 4°C. Cells were harvested by centrifugation at 1500×*g* for 15 min and the pellet was washed with 200 ml of distilled water per 1 l culture. After centrifugation (2000×*g* for 10 min), the pellets were flash-frozen on dry ice/ethanol and stored at −70°C. A purification protocol similar to that for NF-κB P50 was used [11]. Briefly, cells from 1 l culture were resuspended in 30 ml buffer A (10 mM HEPES pH 7.5, 400 mM NaCl, 10 mM DTT, 5% glycerol, 1 μg/ml leupeptin, 1 μg/ml pepstatin, 0.5 mM PMSF) and lysed by sonication. The cell debris was removed by centrifugation (33 000×*g* for 30 min). The DNA was precipitated by addition of 1.8 ml 10% w/v polyethylene imine, stirring for 15 min, and centrifugation at 23 000×*g* for 30 min. To the supernatant, sat-

*Corresponding author. Fax.: (33) (476) 207199.
E-mail: mueller@embl-grenoble.fr

Abbreviations: BSA, bovine serum albumin; DLS, dynamic light scattering; DTT, dithiothreitol; EMSA, electrophoretic mobility shift assay; ESRF, European Synchrotron Radiation Facility; FPLC, fast protein liquid chromatography; HIV, human immunodeficiency virus; IPTG, isopropyl-β-D-thiogalactopyranoside; MES, 2-[*N*-morpholino]ethanesulfonic acid; NLS, nuclear localization signal; PEG, polyethylene glycol; PMSF, phenylmethyl sulfonyl fluoride; RHR, Rel homology region.

PII S0014-5793(97)00217-2

urated ammonium sulfate solution was added to a concentration of 45% saturation and the precipitate removed by centrifugation (25 min at 23000×*g*). Saturated ammonium sulfate solution was further added to a final concentration of 53% saturation followed by stirring for 30 min. After centrifugation (25 min at 23000×*g*), the pellet was redissolved in 50 ml buffer B (buffer A without NaCl) and loaded on a pre-equilibrated 3 ml FAST-SP-Sepharose column (Pharmacia) at a flow rate of 0.5 ml/min. After washing with 50 ml buffer B, NF-κB P52 was eluted with a linear gradient of NaCl (0–1 M, 8 column volumes in total) at a concentration of approx. 0.3 M NaCl. The peak fractions were analyzed by SDS-PAGE. Fractions containing mainly NF-κB P52 were pooled, concentrated to a volume of 300 μl using Centricon-10 (Amicon), and loaded on a Superose-12 gel filtration column (FPLC system, Pharmacia) in buffer C (10 mM HEPES pH 7.5, 100 mM NaCl, 5 mM $MgCl_2$, 3 mM DTT) at a flow rate of 0.5 ml/min. Peak fractions were concentrated to 20 mg/ml and stored at 4°C.

2.2. Site-directed mutagenesis

Introduction of a stop codon (TGA) at amino acid position 330 was carried out using the 'Ex-site' site-directed mutagenesis kit (Stratagene) essentially following the manufacturer's instructions. Pfu DNA polymerase (Stratagene) was used instead of T7 DNA polymerase. The sequences of the primers used were 5′-TCACACCAGAGGGTAATAGGTGAACTGTTTGG and 5′-GACAAGGAAGAGGTGCAGCGGAAGCGG (mutant triplet underlined). The sequence at the site of mutation was confirmed by DNA sequencing and the purified mutant protein was characterized by N-terminal automated Edman degradation and electrospray mass spectroscopy.

2.3. Sample characterization

Dynamic light scattering was performed with a DP-801 instrument (Protein Solutions) at concentrations of 5 mg/ml. Binding of pure protein to short DNA duplexes containing the specific κB binding site MHC H-2 (Fig. 2) was confirmed by electrophoretic mobility shift assay (EMSA) using 5% acrylamide gels and stoichiometric amounts of protein and DNA at concentrations of 1–5 μM. DNA and protein bands were visualized by subsequent ethidium bromide and Coomassie Blue staining, respectively. Protein concentration was measured using the Bradford method (Protein Assay, Biorad). To obtain a standard, protein concentration was determined by UV absorption using a theoretical extinction coefficient of $\varepsilon = 19090\ M^{-1}\ cm^{-1}$ calculated from the primary structure according to the method of Gill et al. [12].

2.4. DNA purification

Oligonucleotides were synthesized chemically and subsequently purified by anion exchange chromatography using a Mono-Q HR 10/10 column (FPLC system, Pharmacia). The oligonucleotides were eluted with a linear gradient of NaCl (0.4–0.7 M), fractions were pooled and dialyzed against demineralized water. Dialysis tubing of 3.5 kDa molecular weight cut-off was used (Spectrapore). The solutions were lyophilized and the oligonucleotides were dissolved in demineralized water to give concentrations of 20 mg/ml. Solutions of complementary strands were mixed in equimolar amounts in buffer C to give a final concentration of 10 mg/ml. The DNA was annealed in a water bath which was cooled down from 90°C to room temperature over several hours.

2.5. Crystallization and crystal freezing

NF-κB P52 homodimer:DNA complexes were reconstituted by mixing solutions of 290 μM (20 mg/ml) P52 homodimer in buffer C and 10 mg/ml DNA duplex in a molar ratio of 1:1.2 (excess of DNA) and incubating at room temperature for 5 min. Crystallization trials were carried out at 20°C using the hanging drop vapor diffusion method. Hanging drops containing 1 μl of complex solution and 1 μl of precipitant solution were equilibrated against the precipitant solution in the well. Crystals were harvested in freshly prepared precipitant solution and were then soaked sequentially for 30 min each in solutions containing additionally 2, 4, 8, 16 and 30% PEG 400 as cryoprotectant. To transform crystals of form 5 to the highly diffracting form 5*, the soaking solutions additionally contained 0.5 mM $Yb(NO_3)_3$ (compare Section 3.2). Soaked crystals were suspended in cryo loops of 0.5–0.7 mm diameter (Hampton Research), mounted on a goniometer head and frozen at 100 K in a stream of nitrogen using an Oxford cryosystem.

2.6. Data collection and processing

Diffraction data collection was carried out at 100 K using an oscillation range of 1.0°. Data were collected on the ESRF beamlines ID13 and BM14 using wavelengths of 0.689 and 0.95 Å for crystal forms 5 and 5*, respectively. MAR Research detectors were used for both experiments. Data were processed using the programs DENZO and SCALEPACK [13].

3. Results

3.1. Co-crystallization of NF-κB P52 with DNA fragments

Complementary pairs of oligonucleotides with lengths ranging from 11- to 22-mers were designed to form a total of 42 DNA duplexes with blunt, 5′- or 3′-overhanging ends. All resulting DNA fragments contained the natural κB binding site MHC H-2 which is the preferred site for P52 homodimers ([8], Fig. 2). Freshly prepared protein samples were monodisperse and active in binding to specific DNA as determined by dynamic light scattering and EMSA, respectively. In addition to crystallization screens performed with the 'Natrix' reagents (Hampton Research), two-dimensional grid screens of pH (pH values 4.7, 5.6, 6.0, 6.5, 7.0 and 8.0) against PEG of various

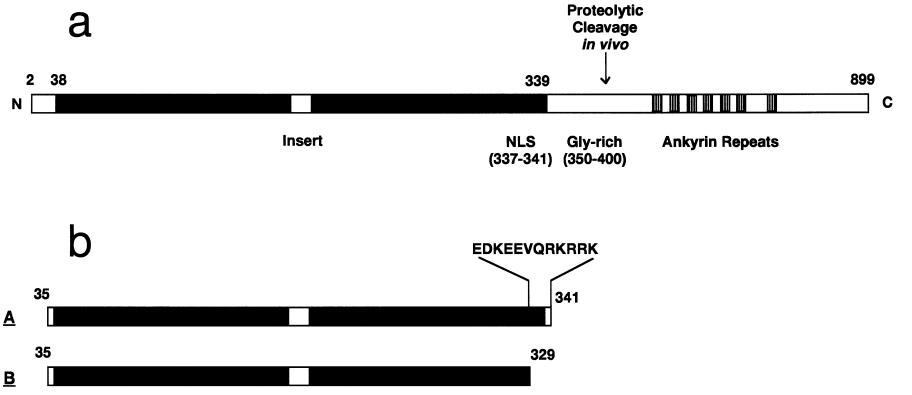

Fig. 1. (a) Schematic representation of human NF-κB P100, the cytoplasmic precursor of NF-κB P52. Black bars indicate the Rel homology region (RHR); the nuclear localization signal (NLS) is located at the C-terminal end of the homology region. The RHR is interrupted by an insert. The C-terminal region contains seven ankyrin repeats and is separated from the RHR by a glycine-rich stretch. (b) NF-κB P52 constructs used for co-crystallization. Construct A contains the entire Rel homology region but misses the N- and C-terminal tails. The highly charged sequence of the C-terminal tail containing the NLS is indicated (one-letter amino acid code). These residues are flexible in the NF-κB P50:DNA co-crystal structures and have been removed in construct B.

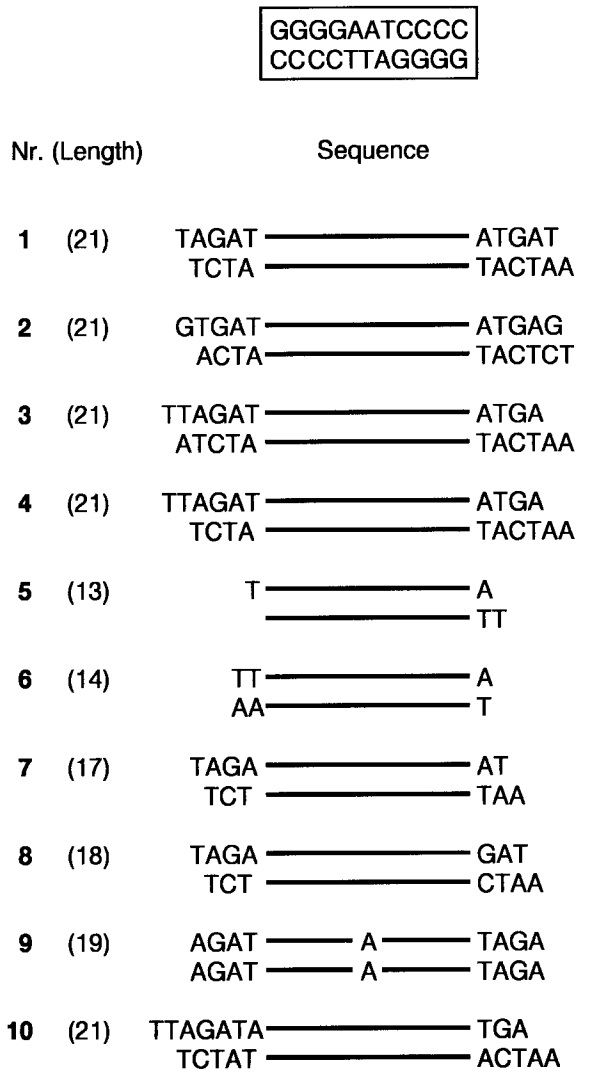

Fig. 2. Sequence of the 10 DNA duplexes which gave co-crystals. The box contains the natural 11-base pair κB binding site MHC H-2 which is subsequently indicated as two solid lines. The numbering corresponds to that used for the crystal forms listed in Table 1. The length of the oligonucleotide is given in parentheses. Top strands are denoted in the 5′→3′ direction. DNA fragment 9 contains a central A:A mismatch and 4 mismatches at either end. It corresponds to the DNA duplex used in co-crystallization of human NF-κB P50 [1].

concentrations and molecular weights (400, 600, 3K, 4K, 6K and 8K) were used. NF-κB P52 protein construct A which contains the entire RHR (residues 35–341, Fig. 1b) yielded co-crystals with four different DNA duplexes (forms 1–4, Table 1 and Fig. 2). Interestingly, all crystal forms contained relatively long DNA fragments (21-mers). The crystallization conditions were very similar with the exception of form 4 which grew at higher pH (pH 6.5). However, none of these forms was suitable for further analysis due to low reproducibility (form 1), high mosaicity (form 2) or weak diffraction (form 3, 4).

3.2. Protein engineering improves co-crystal quality

The initial construct A contained the entire RHR without the flexible N- and C-termini which in the case of NF-κB P50 could be cleaved off proteolytically. However, a C-terminal segment of the RHR appears to be flexible in both P50 homodimer:DNA co-crystal structures [1,2]. Residues 353–366 of human NF-κB P50, 14 mostly charged residues comprising the NLS, are invisible in the electron density maps. Tyr-351 in human NF-κB P50 (Tyr-326 in NF-κB P52) is the last residue involved in secondary structure interactions of the C-terminal Ig-domain (β-strand g). We suspected that an equivalent tail in NF-κB P52 might interfere with the formation of well-ordered co-crystals and that it could be removed without disrupting structurally important interactions. Therefore, in a second protein construct (B, amino acids 35–329, Fig. 1b), 12 mostly charged amino acid residues (330-EDKEEVQRKRRK-341) were truncated from the C-terminus by introduction of a STOP codon at amino acid position 330 of the gene (see Section 2.2). This protein variant was strongly expressed and showed high solubility. Crystallization screens followed by refinement of the initial conditions quickly led to six new crystal forms containing DNA fragments of various lengths (forms 5–10, Table 1 and Fig. 2). In contrast to protein variant A, co-crystals with shorter DNA fragments (13-, 14-, 17-, 18- and a 19-mer) could be obtained. Apart from the 14-mer, all DNA duplexes contained overlapping ends. All crystal forms were grown at pH 6.0 with the exception of crystal form 10 which was grown at pH 5.6. Other common features are the presence of 5–50 mM Mg^{2+} and the use of PEG of molecular weights ranging from 3000 to 8000 as precipitant. Five out of these six crystal forms showed weak diffraction with the maximum resolution ranging from 8.0 to 4.5 Å and were therefore unsuitable for structure determination. However, crystal form 5, bearing a 13-mer with two 5′-T overlapping ends showed anisotropic diffraction to 2.4 Å resolution in two directions and to 3.4 Å in the third direction. This form grew within 4–5 days to a maximum size of $800\times300\times120$ μm^3 using a mixture of 50 mM MES pH 6.0, 5 mM $MgSO_4$, 4–6% PEG 4000 and 5 mM DTT as reservoir solution. To further improve crystal quality, a DNA duplex was constructed in which one of the terminal thymines was replaced by an adenine. Provided the DNA duplexes stack end-on in the crystal, this should allow formation of a Watson/Crick base pair by concomitant ends. However, this DNA fragment did not yield any co-crystals.

3.3. Diffraction analysis and transformation to a highly diffracting co-crystal form

As determined from frozen crystals, form 5 belongs to space group $I2_12_12_1$ with unit cell dimensions $44.5\times129.4\times131.9$ Å^3. Freezing did not change the unit cell parameters significantly (data not shown). Variations in the lengths of unit cell axis *b* and *c* up to ±2 Å were observed with different crystals whereas the *a*-axis did not show significant variability. The Matthews constant $V_M = 2.54$ Å^3/Da is consistent with 1/2 complex per asymmetric unit and a solvent content of 51.6% [14]. A 79.6% complete dataset to 3.8 Å resolution has been collected at 100 K on the microfocus beamline ID13 at the ESRF in Grenoble, France (Table 2). The small size of the beam (30 μm^2) allowed us to translate the crystal several times. This procedure limited radiation damage which occurred despite data collection at low temperature. Two observations indicate that the crystallographic *a*-axis corresponds to the direction of the DNA helical axis in the crystal. First, the length of the *a*-axis (44.5 Å) does not vary with different crystals and corresponds to the theoretical length

Table 1
Co-crystal forms of NF-κB P52 with various DNA fragments

Crystal form[a]	DNA length[a]	pH[b]	Crystallization conditions[c]		Max. size (μm³)	Diffraction limit (Å)[d]
			Salt(s)	Precipitant		
Protein construct A						
1	21	4.7	80 mM $MgCl_2$	14% PEG 3K	400×130×110	3.5[e]
2	21	4.7	80 mM $MgCl_2$	12% PEG 3K	400×200×150	4.0
3	21	4.7	60 mM $MgCl_2$	10% PEG 3K	200×150×60	8.0
4	21	6.5	10 mM $MgCl_2$ 100 mM NH_4OAc	10% PEG 4K	300×100×50	5.5
Protein construct B						
5/5*	13	6.0	5 mM $MgSO_4$	5% PEG 4K	800×300×120	2.4/<2.0[f]
6	14	6.0	5 mM $MgSO_4$	5% PEG 4K	800×100×50	4.5
7	17	6.0	5 mM $MgCl_2$ 150 mM $(NH_4)_2SO_4$	15% PEG 8K	200×80×80	7.0
8	18	6.0	5 mM $MgCl_2$ 200 mM $(NH_4)_2SO_4$	14% PEG 8K	500×80×80	5.5
9	19	6.0	50 mM $MgCl_2$	15% PEG 3K	120×120×80	8.0
10	21	5.6	20 mM $MgCl_2$ 50 mM $(NH_4)_2SO_4$	13% PEG 3K	500×100×30	8.0

[a]The sequence of the DNA duplexes is shown in Fig. 2. The numbers of the crystal forms correspond to the numbers used therein. The DNA length is given in number of bases.
[b]For crystallization at pH 4.7 (crystal form 1–3), 50 mM NaOAc was used as a buffer. For crystal form 4–10, 50 mM MES was used.
[c]The concentrations cited are those in the reservoir solution. For crystal form 1–3, 2 mM spermine was used as additive.
[d]Crystal form 2–4, rotating anode; crystal form 1, 5–10, synchrotron radiation.
[e]Space group $P2_{(1)}2_{(1)}2_{(1)}$ with unit cell axis $a=73$ Å, $b=82$ Å and $c=146$ Å, 1 complex/asymmetric unit.
[f]Crystal form 5 diffracted anisotropically to 2.4 Å in two and to 3.4 Å in the third direction. After transformation to the highly diffracting form 5*, reflections are observed beyond 2.0 Å in all directions (Fig. 3b).

of a B-form DNA 13-mer (44.2 Å). Second, strong streaks at a Bragg spacing of 3.3–3.4 Å (corresponding to one base step) resulting from helical diffraction can be observed perpendicular to the *a*-axis (compare Fig. 3). Interestingly, along the direction of the *a*-axis, the lowest resolution is observed which might indicate imperfect end-on stacking of the DNA fragments in the crystal. We intended to overcome the limitations of anisotropic diffraction by soaking heavy metal ions into the crystal which can have a stabilizing effect. In initial trials, crystals soaked as described in Section 2.5 in solutions containing PEG 400 and additionally 0.5 mM $Yb(NO_3)_3$ normally cracked. Surprisingly, fragments of crystals treated in that way showed isotropic diffraction beyond 3 Å resolution using X-rays from a rotating anode. Further investigation showed that a transformation of the crystal lattice occurred during soaking when concentrations of 20–30% PEG 400 were reached. Increasing the concentration of PEG 400 very slowly from 15% onwards often allowed crystal transformation with limited damage. Rapid macroscopic shrinking of the crystal along the *b*-axis could be followed under the microscope, impressively demonstrating the ongoing transformation. Using synchrotron radiation, successfully transformed crystals diffract beyond 2.0 Å resolution (Fig. 3). Crystals transformed to this highly diffracting form (form 5*) belong to space group $P2_12_12_1$ with a considerably shorter *b*-axis and a slightly longer *c*-axis (unit cell dimensions 44.2×121.0×134.9 Å³). In contrast to the non-transformed crystal form 5, the asymmetric unit is occupied by one complex and the solvent content is reduced to 48.7% ($V_M=2.40$ Å³/Da). A complete dataset to 2.1 Å resolution with $R_{sym}=6.1\%$ on intensities was collected on BM14 at the ESRF from one crystal (Table 2). The crystal diffracted to a resolution better than 2.0 Å at the beginning of the data collection. However, radiation damage restricted the data collection to 2.1 Å resolution. The reasons for the dramatic improvement of diffraction quality after space group transformation are presently unknown. However, structure solution in both space groups will allow investigation of molecular rearrangements and changes in crystal contacts which give rise to the improved crystal packing.

4. Discussion

Some general rules for protein:DNA co-crystallization conditions have been established [15]. These include near neutral to acidic pH, the presence of divalent and/or polyvalent cations and the use of PEG alone or in combination with salts as precipitants. Our results conformed to these general rules. All crystal forms were grown at neutral to acidic pH (pH 6.5–4.7), in the presence of Mg^{2+} ions and using PEG 3000, PEG 4000 or PEG 8000 as precipitant (Table 1).

Table 2
Summary of diffraction data statistics

Crystal form	5	5*
Space group	$I2_12_12_1$	$P2_12_12_1$
Resolution (Å) (highest resolution shell)	20.0–3.8 (3.9–3.8)	20.0–2.1 (2.2–2.1)
No. of measured reflections	10438	124281
No. of unique observations	3177 (290)	39642 (4127)
Redundancy	3.3	3.1
Completeness (%)	79.9 (75.9)	91.8 (78.1)
R_{sym} (%)[a]	10.2 (25.3)	6.1 (31.2)

[a]$R_{sym}=\Sigma|I_i-\langle I_i\rangle|/\Sigma|\langle I_i\rangle|$, where I_i is the intensity of the individual reflection and $\langle I_i\rangle$ is the mean value of its equivalent reflections. Values given in parentheses correspond to the highest resolution shells.

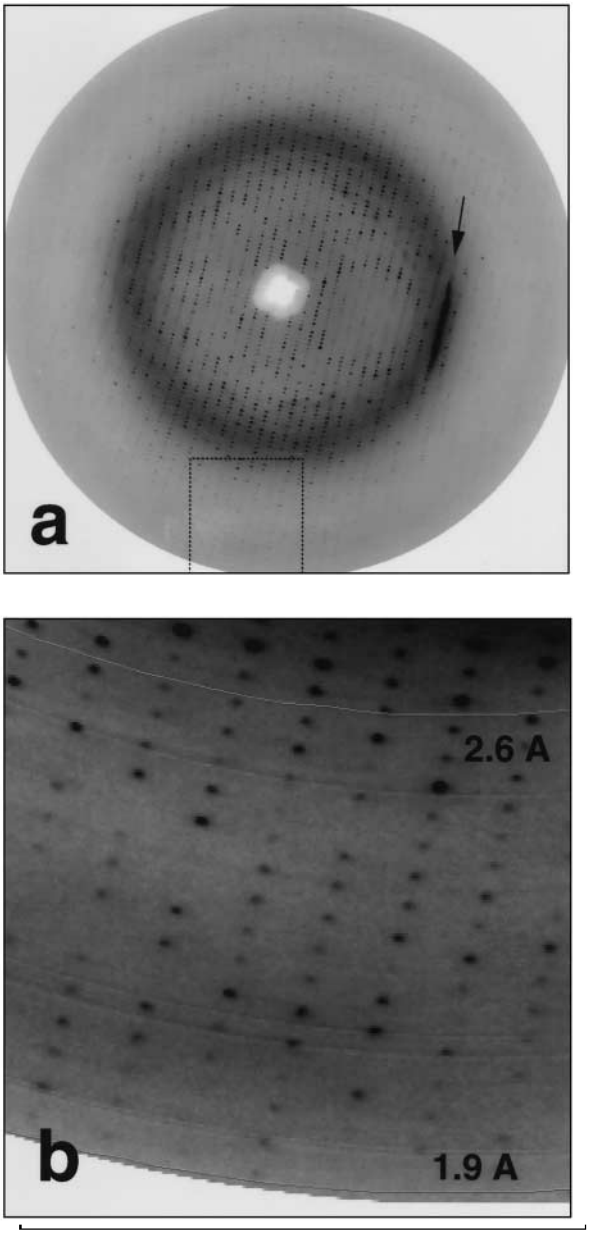

Fig. 3. (a) 1° oscillation diffraction image of NF-κB P52 homodimer:DNA co-crystal form 5*. The picture was taken with an MAR Research detector at BM14 of the ESRF using a wavelength of λ = 0.95 Å. The exposure time was 90 s. The arrow indicates a strong streak perpendicular to the *a*-axis at a Bragg spacing of 3.3–3.4 Å. Due to the alignment of the crystal, the symmetry-related pattern is not recorded. (b) A close-up of the high-resolution area indicated by dashed lines in (a) shows reflections up to 1.9 Å resolution.

Our results lead to two conclusions concerning future co-crystallization of Rel family proteins with DNA. First, the use of relatively short DNA fragments is advantageous. The best co-crystal form was obtained with the shortest DNA fragment. Interestingly, the two known co-crystal structures of the NF-κB P50 homodimer:DNA complex also contain relatively short fragments of ordered B-DNA (10 and 11 base pairs, respectively). These observations can probably be explained by the overall shape of the complex. Perpendicular to the DNA helical axis the protein dimer has dimensions of approx. 80 Å by 100 Å while along the DNA axis the protein dimer width is only approx. 45 Å, corresponding to the length of a 12- or 13-mer of B-DNA. Consequently, longer DNA duplexes stick out of the relatively flat protein dimer and thus can prevent formation of protein-protein contacts in the direction of the DNA which are essential for tight crystal packing. Second, the optimal borders for a Rel protein construct appear to be at the beginning of the N-terminal end of the RHR and 10 amino acid residues before the C-terminal end of the RHR. Based on the two crystal structures of NF-κB P50, the C-terminus of NF-κB P52 was further truncated to end two residues after the last residue involved in a secondary structure element. Limited proteolysis is a useful tool to define protein domain borders but the obtained results are biased by sequence specificity and probe radius of the protease. The knowledge of the three-dimensional structure of a homologous protein allowed us to engineer the construct more precisely than we were able to do it based only on proteolysis data. Because of the high sequence conservation within the RHR, the optimized construct size described in this work could most probably be used in co-crystallization of other Rel proteins with DNA.

In our system, engineering the protein and the DNA fragment in combination with screening of different crystallization conditions has been a successful approach. The crystallization process crucially depends on macromolecular surface properties which define possible packing arrangements. Flexible parts, steric bulges and charge clusters on the surface can prevent the formation of well-ordered crystals. In this study, changing these surface properties by engineering the components of the macromolecular complex has led to diffraction-quality co-crystals. Determination of the structure of the NF-κB P52 homodimer:DNA complex is now underway.

Acknowledgements: The plasmid containing the NF-κB P52 (35–341) gene encoding for construct A was kindly provided by C.L. Larson and G. Verdine (Harvard University). We would like to thank F. Baudin (EMBL Grenoble) for advice on site-directed mutagenesis. Also, we would like to thank A. Thompson (EMBL Grenoble) for help at BM14 and A. Brahm and C. Riekel for help at ID13 at the European Synchrotron Radiation Facility (ESRF) in Grenoble, France. We would also like to thank R. Eritja (EMBL Heidelberg) for oligonucleotide synthesis.

References

[1] C.W. Müller, F.A. Rey, M. Sodeoka, G.L. Verdine, S.C. Harrison, Nature 373 (1995) 311–317.
[2] G. Ghosh, G. Van Duyne, S. Ghosh, P.B. Sigler, Nature 373 (1995) 303–310.
[3] P.A. Baeuerle, T. Henkel, Annu. Rev. Immunol. 12 (1994) 141–179.
[4] P.A. Baeuerle, D. Baltimore, Cell 87 (1996) 13–20.
[5] C. Barillas-Mury, A. Charlesworth, I. Gross, A. Richman, J.A. Hoffmann, F.C. Kafatos, EMBO J. 15 (1996) 4691–4701.
[6] T.D. Gilmore, P.J. Morin, Trends Genet. 9 (1993) 427–433.
[7] C.W. Müller, S.C. Harrison, FEBS Lett. 369 (1995) 113–117.
[8] R.M. Schmid, S. Liptey, J.C. Betts, G.J. Nabel, J. Biol. Chem. 269 (1994) 32162–32176.
[9] J. Pan, R.P. McEver, J. Biol. Chem. 270 (1995) 23077–23083.
[10] M. Sodeka, C.J. Larson, L. Chen, K.P. LeClair, G.L. Verdine, Biomed. Chem. Lett. 3 (1993) 1089–1094.
[11] M. Sodeka, C.J. Larson, L. Chen, W.S. Lane, G.L. Verdine, Biomed. Chem. Lett. 3 (1993) 1095–1100.
[12] S.C. Gill, P.H. Von Hippel, Anal. Biochem. 182 (1989) 319–326.
[13] Otwinowsi, Z. (1991) DENZO. A Film Processing Program for Macromolecular Crystallography, Yale University, New Haven, CT.
[14] B.W. Matthews, J. Mol. Biol. 33 (1968) 491–497.
[15] A. Joachimiak, P.B. Sigler, Methods Enzymol. 208 (1991) 82–99.